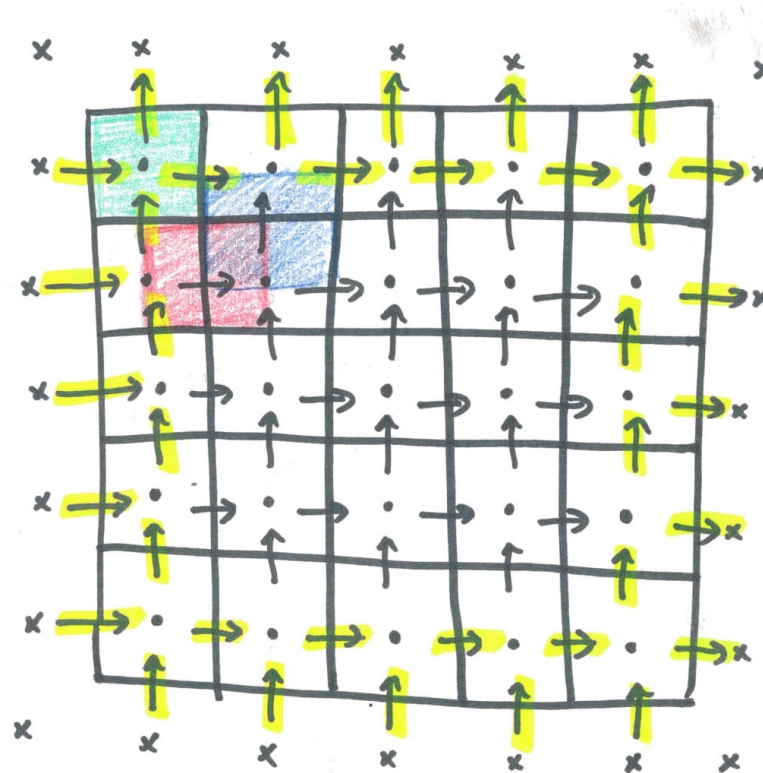


Problem 1

A two-dimensional cavity is filled with an incompressible Newtonian fluid. The fluid is driven by the lid moving with a constant velocity U . The cavity has dimensions $H \times H$. Find the steady state solution.



- = interior pressure point
- x = exterior pressure point
- \rightarrow = u-velocity point
- \uparrow = v-velocity point
- = u,v points along boundary
- = first interior u-velocity control area
- = first interior v-velocity control area
- = first interior pressure control area

Figure 1: Domain partition with rectangular velocity meshes.

(a) Describe the essential steps for the projection method in physical terms.

0.1 Projection Method

For the Domain $H = 1$ with N points on the collocated grid, the staggered grid will have u -velocity with size $[N]$ in x and $[N+1]$ in y , v -velocity with size $[N+1]$ in x and $[N]$ in y , and pressure p with size $[N+1]$ in x and y (Fig.1).

Step 1. Compute the intermediate velocities u^* and v^* explicitly using the u -momentum and v -momentum equations by ignoring the pressure gradient term.

$$u^* = u^n + \Delta t(D_u - A_u) \quad (1)$$

$$v^* = v^n + \Delta t(D_v - A_v) \quad (2)$$

A_u , A_v are the advective terms of the u -momentum, v -momentum discretizations.

$$A_u = \frac{\partial u^2}{\partial x} + \frac{\partial uv}{\partial y} = \frac{1}{h} (u_E^2 - u_W^2 + u_N v_N - u_S v_S) \quad (3)$$

$$A_v = \frac{\partial uv}{\partial x} + \frac{\partial v^2}{\partial y} = \frac{1}{h} (u_E v_E - u_W v_W + v_N^2 - v_S^2) \quad (4)$$

The u -momentum interpolated variables for advective terms:

$$\begin{aligned} u_P &= u_{i,j} \\ u_E &= \frac{1}{2}(u_{i,j} + u_{i+1,j}) \\ u_W &= \frac{1}{2}(u_{i,j} + u_{i-1,j}) \\ u_N &= \frac{1}{2}(u_{i,j} + u_{i,j+1}) \\ u_S &= \frac{1}{2}(u_{i,j} + u_{i,j-1}) \\ v_N &= \frac{1}{2}(v_{i+1,j} + v_{i,j}) \\ v_S &= \frac{1}{2}(v_{i+1,j-1} + v_{i,j-1}) \end{aligned}$$

The v -momentum interpolated variables for advective terms:

$$\begin{aligned} v_P &= v_{j,i} \\ v_E &= \frac{1}{2}(v_{i,j} + v_{i+1,j}) \\ v_W &= \frac{1}{2}(v_{i,j} + v_{i-1,j}) \\ v_N &= \frac{1}{2}(v_{i,j} + v_{i,j+1}) \\ v_S &= \frac{1}{2}(v_{i,j} + v_{i,j-1}) \\ u_E &= \frac{1}{2}(u_{i,j+1} + u_{i,j}) \\ u_W &= \frac{1}{2}(u_{i-1,j+1} + u_{i-1,j}) \end{aligned}$$

D_u, D_v are the diffusive terms of the u -momentum, v -momentum discretizations.

$$D_u = \frac{1}{Re} \left(\frac{\partial^2 u}{\partial x^2} + \frac{\partial^2 u}{\partial y^2} \right) = \frac{1}{Re} \left(\frac{u_E + u_W + u_N + u_S - 4u_P}{h^2} \right) \quad (5)$$

$$D_v = \frac{1}{Re} \left(\frac{\partial^2 v}{\partial x^2} + \frac{\partial^2 v}{\partial y^2} \right) \frac{1}{Re} \left(\frac{v_E + v_W + v_N + v_S - 4v_P}{h^2} \right) \quad (6)$$

The u -momentum variables for diffusive terms:

$$\begin{aligned} u_P &= u_{i,j} \\ u_E &= u_{i+1,j} \\ u_W &= u_{i-1,j} \\ u_N &= u_{i,j+1} \\ u_S &= u_{i,j-1} \end{aligned}$$

The v -momentum variables for diffusive terms:

$$\begin{aligned} v_P &= v_{j,i} \\ v_E &= v_{i+1,j} \\ v_W &= v_{i-1,j} \\ v_N &= v_{i,j+1} \\ v_S &= v_{i,j-1} \end{aligned}$$

Step 2. The intermediate velocities are used in the Poisson pressure equation to calculate the updated pressure field.

$$\frac{\partial^2 p}{\partial x^2} + \frac{\partial^2 p}{\partial y^2} = \frac{1}{\Delta t} \left(\frac{\partial u^*}{\partial x} + \frac{\partial v^*}{\partial y} \right) \quad (7)$$

Central differences is applied to the Poisson pressure equation and p_P is solved for to compute the pressure at the next time step.

LHS:

$$\frac{(\Delta y)^2(p_E + p_W - 2p_P) + (\Delta x)^2(p_N + p_S - 2p_p)}{(\Delta x)^2(\Delta y)^2} \quad (8)$$

RHS:

$$\frac{1}{\Delta t} \left(\frac{\Delta y(u_E - u_W) + \Delta x(v_N - v_S)}{\Delta x \Delta y} \right) \quad (9)$$

$\Delta x = \Delta y = h$:

$$p_P^{n+1} \leftarrow \frac{1}{4}(p_E^n + p_W^n + p_N^n + p_S^n) - \frac{h}{\Delta t}(u_E^* - u_W^* + v_N^* - v_S^*) \quad (10)$$

We now derive the over-relaxation method via $p_\omega(x, y) = (1 + \omega)p'(x, y) - \omega p(x, y)$, which has an optimal value of $\omega = 0.9$.

$$p_P^{n+1} \leftarrow \frac{1 + \omega}{4}(p_E^n + p_W^n + p_N^n + p_S^n) - \frac{h(1 + \omega)}{\Delta t}(u_E^* - u_W^* + v_N^* - v_S^*) - \omega p_P^n \quad (11)$$

To combine this method with Gauss-Seidel, the old values are overwritten with the new ones such that $p_W^n \rightarrow p_W^{n+1}$ and $p_N^n \rightarrow p_N^{n+1}$. We use the following quantities for computation:

$$\begin{aligned} p_P &= p_{i,j} \\ p_E &= p_{i+1,j} \\ p_W &= p_{i-1,j} \\ p_N &= p_{i,j+1} \\ p_S &= p_{i,j-1} \\ u_E^* &= u_{i,j}^* \\ u_W^* &= u_{i-1,j}^* \\ v_N^* &= v_{i,j}^* \\ v_S^* &= v_{i,j-1}^* \end{aligned}$$

Step 3. Correct the intermediate velocities u^* , v^* using the updated pressure.

$$u_P^{n+1} = u_P^* - \frac{\Delta t}{h}(p_E^{n+1} - p_W^{n+1}) \quad (12)$$

where $u_P^* = u_{i,j}^*$, $p_E^{n+1} = p_{i+1,j}^{n+1}$, and $p_W^{n+1} = p_{i,j}^{n+1}$.

$$v_P^{n+1} = v_P^* - \frac{\Delta t}{h}(p_N^{n+1} - p_S^{n+1}) \quad (13)$$

where $v_P^* = v_{i,j}^*$, $p_N^{n+1} = p_{i,j+1}^{n+1}$, and $p_S^{n+1} = p_{i,j}^{n+1}$.

Step 4. The staggered grid is mapped to the collocated grid after convergence.

$$u_{final}(i, j) = \frac{1}{2}(u_{i,j} + u_{i,j+1}) \quad (14)$$

$$v_{final}(i, j) = \frac{1}{2}(v_{i,j} + v_{i+1,j}) \quad (15)$$

$$p_{final}(i, j) = \frac{1}{2}(p_{i,j} + p_{i+1,j+1}) \quad (16)$$

0.2 Boundary Conditions

The velocities have no-slip boundary conditions. The u -velocities are zero along the side walls, $x = 0$ and $x = H$. At the bottom of the cavity where $y = 0$, the average of the interior and exterior velocities on the staggered grid must be zero such that:

$$u_{\text{exterior}} = -u_{\text{interior}}$$

At the top of the cavity where $y = H$, the average of the interior and exterior velocities on the staggered grid must be one such that:

$$u_{\text{exterior}} = 2 - u_{\text{interior}}$$

The v -velocities are zero along the bottom and top walls, $y = 0$ and $y = H$. At the sides of the cavity, $x = 0$ and $x = H$, the average of the interior and exterior velocities on the staggered grid must be zero such that:

$$v_{\text{exterior}} = -v_{\text{interior}}$$

Normal to the boundaries, there is no flow such that the pressure outside is equal to the pressure inside. Thus, along each boundary, we have the Neumann boundary condition:

$$p_{\text{exterior}} = p_{\text{interior}}$$

0.3 Divergence Free Constraint

The incompressible Navier-Stokes equation:

$$\frac{\partial \mathbf{u}}{\partial t} + (\mathbf{u} \cdot \nabla) \mathbf{u} = -\frac{1}{\rho} \nabla p + \nu \nabla^2 \mathbf{u} \quad (17)$$

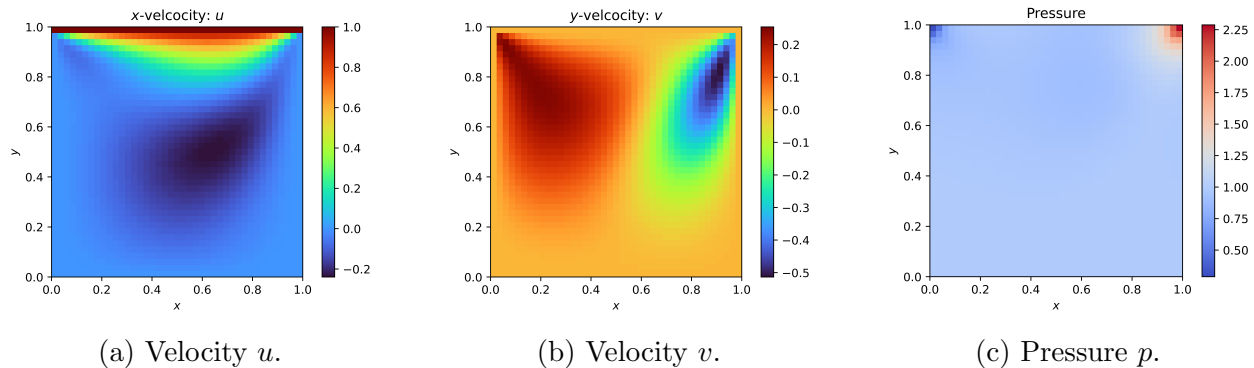
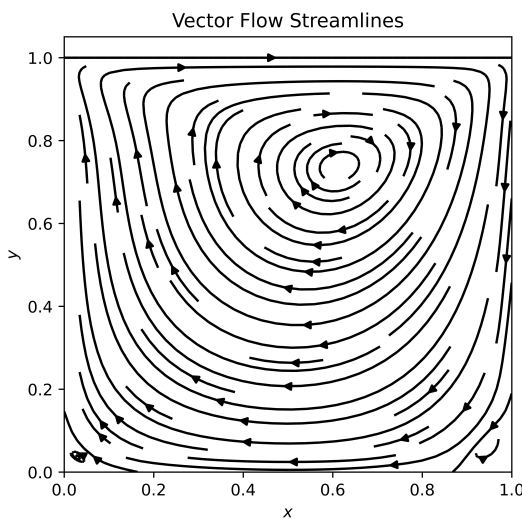
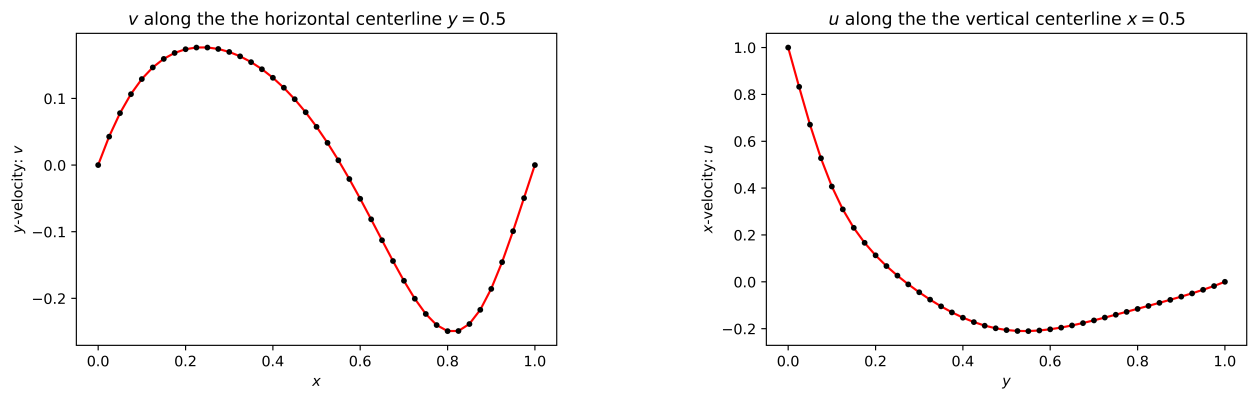
In the projection step of the algorithm, we correct the intermediate velocity to obtain the solution \mathbf{u}^{n+1} :

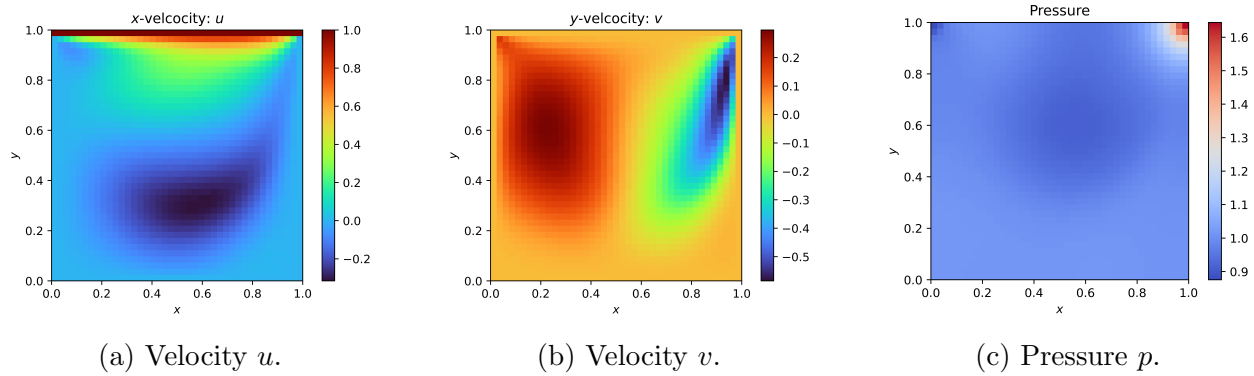
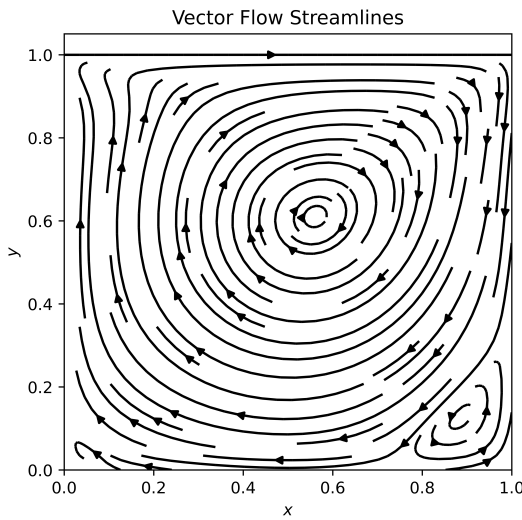
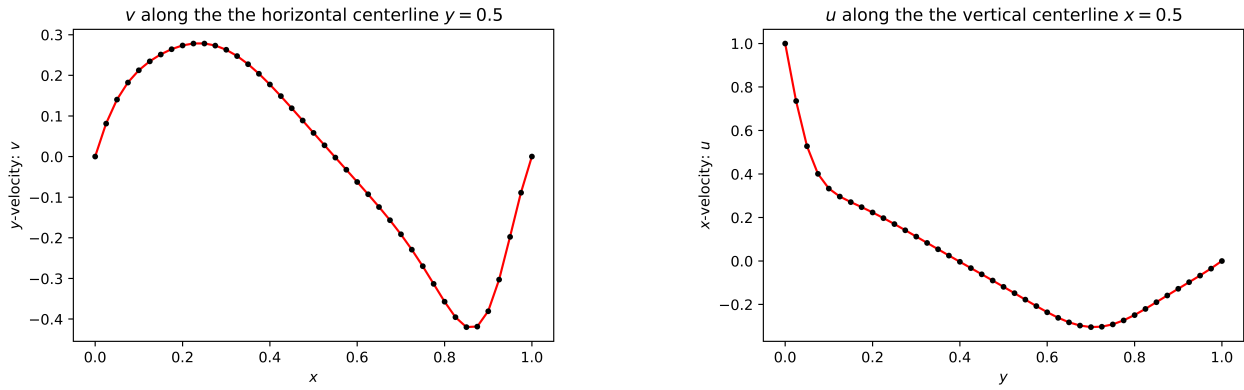
$$\frac{\mathbf{u}^{n+1} - \mathbf{u}^*}{\Delta t} = -\frac{1}{\rho} \nabla p \quad (18)$$

Taking the divergence and requiring that $\nabla \cdot \mathbf{u}^{n+1} = 0$, the divergence (continuity) constraint, we derive the Poisson equation for p^{n+1} :

$$\nabla^2 p^{n+1} = \frac{\rho}{\Delta t} \nabla \cdot \mathbf{u}^* \quad (19)$$

Thus, the Poisson pressure equation in which we solve upholds the divergence free constraint.

Figure 2: Steady state u, v, p grids at $Re = 100$.Figure 3: Steady state streamlines at $Re = 100$.Figure 4: Steady state u and v at $Re = 100$.

Figure 5: Steady state u, v, p grids at $Re = 400$.Figure 6: Steady state streamlines at $Re = 400$.Figure 7: Steady state u and v at $Re = 400$.

(b) Compute the steady state solutions for both $Re = 100$ and $Re = 400$.

0.4 Simulation Criteria

The initial conditions of the simulation are as follows:

Velocity u : $U = 1$ at the lid, zero elsewhere

Velocity v : zero everywhere

Pressure p : $P = 1$ everywhere

Domain $H = 1$

$N = 41$ grid points in either direction

$h = \Delta x = \Delta y = 0.025$

$\Delta t = 0.005$

$\omega = 0.9$

Time steps = 4000

Max SOR Iterations = 1000

The solution converges to steady state within the number of time steps. The convergence of GS/SOR is determined by the maximum of the absolute difference in pressure between the current and the previous iteration. If this value is less than 10^{-4} , it has converged.

0.5 Comparison to Literature

The steady state streamlines for $Re = 100$ (Fig.3) and $Re = 400$ (Fig.6) look similar to those in the resource. From $Re = 100$ to $Re = 400$, the main vortex shifts downward and the vortices in the bottom corners of the cavity become larger.

We define the minimum velocity at the vertical centerline as u_{min} , the minimum velocity at the horizontal centerline as v_{max} , and the maximum velocity at the horizontal centerline as v_{max} (See Figures 4 and 7). These values are compared to the literature values in Table 1, where percent error is defined as:

$$\delta = \frac{|simulation - resource|}{|resource|} \times 100\% \quad (20)$$

Overall, the simulation results are representative of those in the resource. At $Re=100$, the simulation values are accurate with an overall percent error of less than two-percent. On the other hand, at $Re=400$, the simulation values are less accurate with an overall percent error of less than eight-percent. These errors could be improved by reducing truncation error through increasing the grid size. The higher Reynolds solution may have larger percent error because it takes longer to converge and may require smaller criteria for convergence to be more representative of the solution in the resource.

Velocity	Re	Simulation	Resource	% Error
u_{min}	100	-0.21026	-0.21090	0.3%
v_{min}	100	-0.24925	-0.24533	1.6%
v_{max}	100	0.17636	0.17527	0.6%
u_{min}	400	-0.30430	-0.32726	7.0%
v_{min}	400	-0.41989	-0.44993	6.7%
v_{max}	400	0.27838	0.30203	7.8%

Table 1: Comparison of simulation and resource values for u_{min} , v_{min} , and v_{max} .

Resource: Ghia, U. K. N. G., Kirti N. Ghia, and C. T. Shin. “High-Re solutions for incompressible flow using the Navier-Stokes equations and a multigrid method.” *Journal of computational physics* 48.3 (1982): 387-411.

The simulations were executed at $N = \{16, 32, 64\}$ grid points in either direction with a time step = 0.005 and number of time steps = 4000. The following plots show a comparison of velocity profile values u_{min} , u_{min} , and v_{max} with those from the literature.

- (c) **For $Re = 100$ and $Re = 400$, qualitatively show your two velocity profiles are converging to the literature values by considering three different grid sizes with the grid resolution doubled each time.**

The general trend of the plots in Fig.8 is that the minimum and maximum velocities of the centerline plots are nearing the literature values as the grid size N is increased. It is notable that the higher Reynolds solutions require larger N to be as close to the literature result as for the smaller Reynolds solutions. This finding agrees with the differences in magnitude of percent error in Table 1.

- (d) **Numerically compute the spatial convergence rate of your scheme.**

We take the L2 norm over the sum of all differences in velocities u or v between the grids with $N = \{16, 32, 64\}$ points and the solution with 128 grid points as the spatial error measurement. Since the values at the boundaries are constant between solutions, making the differences in solutions zero along the boundary, $(N - 2)^2$ points on the grid provide meaningful data and are used to compute the error.

$$\epsilon|_u = \frac{\sqrt{\sum_{i,j} (u_N - u_{128})_{ij}^2}}{(N - 2)^2} \quad (21)$$

To execute this, the solution of the grid with 128 points is restricted to match the grid sizes $N = \{16, 32, 64\}$. Meaning, the results from the finer grid are interpolated to a coarser grid. A restriction function was created which implements the boundary

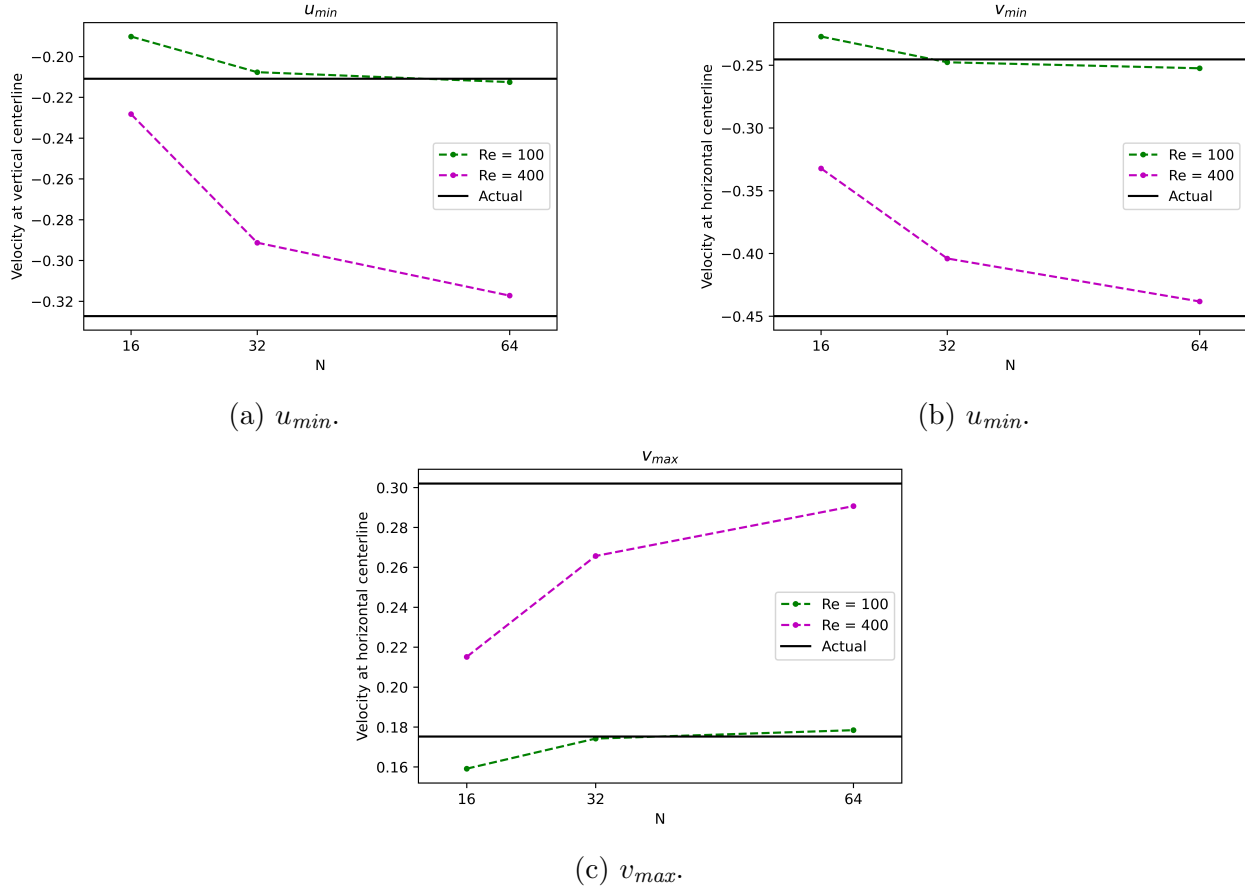
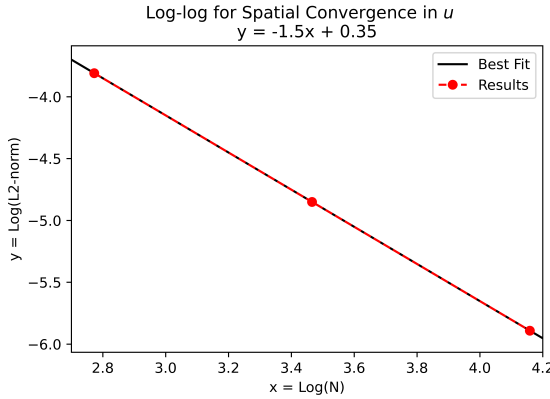
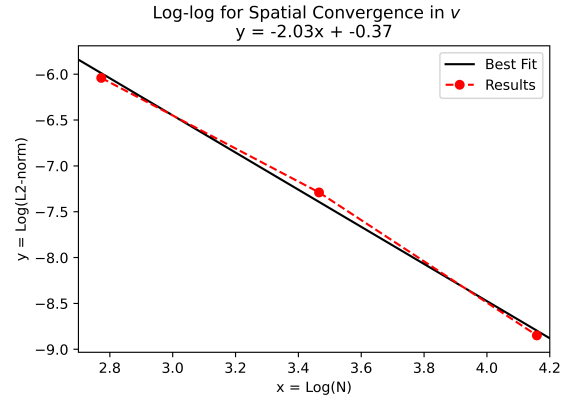
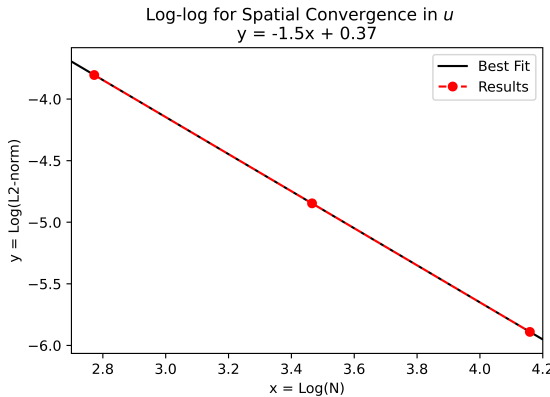
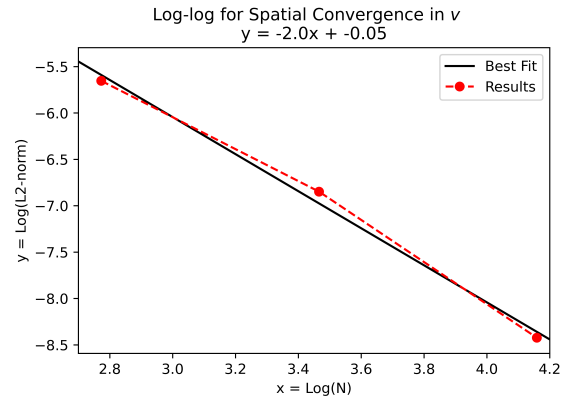


Figure 8: Comparison of velocities from centerline profiles.

conditions for u, v and then averages the 8 fine mesh neighbors of the coarse point ($N, S, E, W, NE, NW, SE, SW$) in 2D, restricting the grid to a $N/2$ mesh. The 128 point grid was first restricted to $N = 64$, then it was recycled into the function to get the restriction at $N = 32$. The function was executed once more to restrict the 128 point grid to $N = 16$. Since the execution time would have taken a day to compute the $N = 128$ grid using the projection method, I substituted the data from the artificial compressibility method.

The spatial convergence rate for v is 2 for $Re = 100$ and $Re = 400$ (Fig. 8). This agrees with what we would expect for the spatial convergence rate when using central differences for the discretization. On the other hand, the convergence rate for u is 1.5, which does not match what is expected based on the discretization.

This signifies that the choice of Reynolds number affects the rate at which the numerical solution spatially converges, such that higher Reynolds number may have a slower spatial convergence rate. This suggests the code has some artifact for u that causes this difference or some discretization implemented was of the first order.

(a) Velocity u , Convergence rate = 1.5.(b) Velocity v , Convergence rate = 2.0.Figure 9: Spatial convergence in u and v at $Re = 100$.(a) Velocity u , Convergence rate = 1.5.(b) Velocity v , Convergence rate = 2.0.Figure 10: Spatial convergence in u and v at $Re = 400$.

- (e) Compare the projection method to the artificial compressibility method from the previous homework with respect to time dependent and time independent flows.

The artificial compressibility method is intended for steady flows because the time derivative is zero at steady state such that the solution satisfies the incompressible equations. Due to this, time-independent governing equations are transformed into time-dependent auxiliary equations. Both this method and the projection method are used to solve time-dependent flow problems. Since, the equations are being solved with respect to time.